Egyptian Journal of Chemistry
http://ejchem.journals.ekb.eg/

Novel p-nitrophenyl Maleanilic Acid and Its Organometallic Chelates of Cr, Mo and W Carbonyls Structure Evaluation Using Different Techniques and Chromium Chelate Cytotoxicity

M.A. Zayed[*1], Khloud R. Oraby [2], Fatma S. M.Hassan[2]

[1]*Chemistry Department, Science Faculty, Cairo University, 12613 Egypt*

[2]*Chemistry Department, Science Faculty, Aswan University, 81528 Egypt*

Abstract

Novel p-nitrophenyl maleanilic acid bidentate free ligand (PNMA) was synthesized eco-friendly by solvent free reaction between 4-nitroaniline and maleic anhydride. Some novel mixed ligand organometallic chelates of formulae [M(CO)4L] (M = Cr , Mo , or W and L = PNMA) were carefully prepared under nitrogen inert gas atmosphere by condensation between ligand PNMA and hexacarbonyl of metal cations Cr , Mo , or W in 1:1 molar ratio. The chemical structures of PNMA free ligand and its novel chelates had been evaluated by elemental analyses, FTIR spectroscopy, 1H-NMR, mass spectroscopy, and thermal analyses (TGA and DTG). The chemical structures of both PNMA free ligand and its chelates were investigated also by XRD technique. The free ligand and its chromium chelate had been evaluated for their anticancer activities against MCF- 7 cells (breast cancer cell line), HCT116 cells (colon cancer cell line) and HepG2 cells (human liver cancer cell line).

Keywords: P-Nitrophenyl Maleanilic Acid, Organometallic Carbonyl Chelates, Antitumor Activity, Spectroscopic Analysis, XRD and Thermal Analysis.

1. Introduction

The synthesis of the novel complexes and metal chelates; in addition to the development of methodologies, particularly for the formation of both of C-M, O-M and N-M bonds are important fields for the synthetic inorganic chemistry. The independent species; which are consisted of a central metal atom or ion bonded with other ions or molecules are known as a coordination complexes or compounds. The formation of these complexes can be identified as Lewis acid / base reactions; in which the central metal atom or ion behaves as a Lewis acid but the surrounding ions or molecules act as Lewis bases. The metal centers can be conveniently assorted using the theory of Pearson Hard-Soft Acid-Base (HSAB) [1]. According to HSAB theory, metal centers with high polarizing potentials are considered hard acids. This theory is not an absolute measure, but it can be considered as a relative scale. It is used to justify experimentally observed tendencies for certain cations to form stable complexes with specific ligand atoms. In our study, according to HSAB theory and ligands denticity [2, 3], p-nitrophenyl maleanilic acid ligand is referred to as bidentate ligand and acts as Lewis base; which coordinated with the Lewis acid metal atom. In this work the Lewis acid metal atom is represented in the form of metal hexa carbonyl. The metal chelates exhibit an enhanced the stability due to presence of chelate rings; when compared with complexes; which containing only monodentate ligands [4]. The conceptual framework of the transition metal carbonyls chemical bonding had been discussed in recent books of both inorganic and organometallic chemistry [5, 6]. It is based on the classic form of the combination of σ and π-back donation between the central metal atom or ion and the ligand according to the model of Dewar-Chatt-Duncanson [7]. The power of Dewar-Chatt-Duncanson model interpreted and prophesied the structure and reactivity of numerous transition metal complexes using both of σ and π-back donation pattern and semiempirical calculations [8, 9].

*Corresponding Author: M.A. Zayed, Tel: 01005776675, mazayed429@yahoo.com
Receive Date: 19 February 2020, Revise Date: 21 March 2020, Accept Date: 03 April 2020
DOI: 10.21608/EJCHEM.2020.24342.2446

Transition metal carbonyl complexes have great attention for the academic research syntheses, because they were serving as precursors for the organometallic complexes preparations. They have significant role in organic syntheses such as hydroformylation and Reppe chemistry [10-14]. Also they were used for industrial purposes as essential homogeneous and heterogeneous catalysts [15]. On the other hand p-nitrophenyl maleanilic acid is an anilic acid because it containing a carboxy group and carboxyanilide (-CO-NH-C6H5) group [16- 21]. Maleanilic acid derivatives are of a senior importance, they can be served as anti-tubercular agents [22] and potential inhibitors [23]. They can act as preventive and therapeutic fungicides [24]. Also they can be used to synthesize the maleimides; which are essential substrates for synthesis the chemical probes for protein structures [18]. They were served as photoinitiators for free-radical polymerization in polymer chemistry and as monomers in the synthesis of both of polymaleimides and copolymers [25, 26].

The objective of this study involved is the synthesis of p-nitrophenyl maleanilic acid ligand (PNMA) using solvent free procedure. The prepared ligand act as the Lewis base donor used to prepare chelates with some hexa carbonyls of group VI transition metals. The instrumental protocols such as elemental analyses, FT-IR spectroscopy, 1H-NMR spectroscopy, mass spectra and finally thermal analyses were applied to characterize the free ligand and its novel metal chelates. Also XRD was studied to test the crystalline structures of the free ligand and its novel chelates. In addition to the study of the thermal stability of the newly synthesized chelates. Finally, PNMA ligand and its chromium complex were screened for their anti-tumor activities versus MCF- 7 cells (breast cancer cell line), HCT116 cells (colon cancer cell line) and HepG2 cells (liver cancer cell line).

2. Experimental

2.1. Materials and Reagents

All the chemicals in this study were of both analytical grade and highest purity available. They included $Cr(CO)_6$, $Mo(CO)_6$, $W(CO)_6$, maleic anhydride and 4-nitroaniline. All the chemicals were obtained from sigma Aldrich (Germany). Organic solvents were absolute ethanol, DMSO and DMF and they were purchased from Alpha Aesar and using them without further purification.

2.2. The Used Instruments

The measurements of weights were performed using sensitive analytical balance [0.0001g, SCALTEC (Germany)]. Melting points were measured using (GallenKamp, Germany) apparatus. Stirring and heating were performed using (VELP) magnetic stirrer theromostated hot plate (Europe). The elemental microanalysis of the purified solid compounds for C, H and N were performed in Cairo University microanalytical Centre. FT-IR measurements were done using Perkin Elmer 1650 spectrophotometer at the wave number region 4000–400 cm^{-1} as KBr disks. ^{1}H-NMR spectroscopy measurements were investigated using Bruker DPX 400 spectrometer (300.06 MHZ) with DMSO as a reference solvent. EI-MS measurements were performed by mass spectrometer of the type Shimadzu Qp-2010 Plus. The measurements of EI-MS were obtained at 70 eV ionizing energy, with 60 µA ionization current and with vacuum being better than 10^{-6} torr. XRD patterns of free ligand and its identical complexes were measured using a diffractometer of the type HZG–4 (Carl Zeiss, Jena) with Ni filtered CuKα radiation. All the XRD measurements were performed at 2θ range of 4°–60° by means of the method of Bragg Brentano and Dicvol 06 program was used for the interpretation of diffractograms. Thermal analyses (TA) of the prepared compounds were performed using Shimadzu system of 30 series TG-50. Mass losses of (1-5 mg) samples and heat response of the change of the samples were measured from 25 up to 700 °C. The rate of heating in an inert nitrogen atmosphere was 10°C/ min. The TA instrument was calibrated by indium as a thermally stable material. The reproducibility of the instruments readings were measured using by running each experiment more than twice.

2.3. Procedures

2.3.1. Synthesis of *p*-nitrophenyl maleanilic acid ligand

P-nitroaniline (0.10 mol, 13.8 g) was mixed with maleic anhydride (0.10 mol, 9.8 g) and grinded in an agate mortar for 52 min at room temperature [27]. During grinding, a nice green powder produced. The solid product was purified and recrystallized from ethanol; then it was dried under vacuum over P_2O_5. The yield was 89 %. This practical work was performed according to the procedures in Scheme (1).

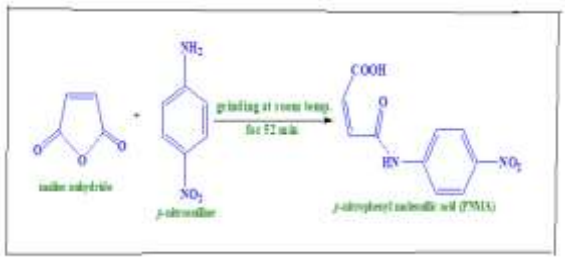

Scheme 1: Synthesis of *p*-nitrophenyl maleanilic acid (PNMA)

2.3.2. Synthesis of metal carbonyl chelates

Novel metal carbonyl mixed ligand chelates of the type of $[M(CO)_4L]$ [M = Cr, Mo or W and L = PNMA = *p*-nitrophenyl maleanilic acid] were synthesized by dissolving PNMA ligand (0.5 m mol, 0.118 g) in least amount of DMF and then $M(CO)_6$ (0.5 m mol) in the same solvent was added. The solution volume was completed to 20 mL with DMF solvent. The obtained reaction mixture was stirring for 60 minutes at 90-100 ºC under reflux in an inert nitrogen atmosphere. Then the obtained product was separated and washed thoroughly with ethanol several times. After that it was recrystallized from the mixture solvent of DMF / ethanol. Finally it was dried using a desiccator containing P_2O_5. The proposed procedures are presented in scheme (2) in accordance with Cooper et al methods modification [28, 29].

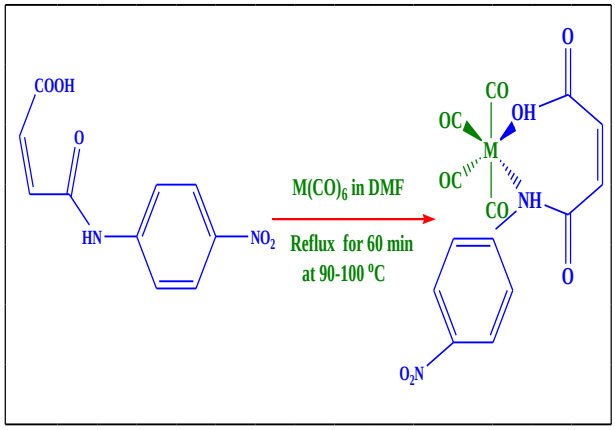

Scheme 2: Synthesis of $[M(CO)_4L]$ chelates (L = PNMA).

2.4. Cytotoxicity

Compound	Mol. Formula	m/z	Color	M.P °C	%C Calc. (found)	%H Calc. (found)	%N Calc. (found)
L = NPMA	$C_{10}H_7O_5N_2$	235.18	Green	210-212	51.07 (50.45)	3.39 (3.71)	11.86 (10.6)
$[Cr(CO)_4L]$	$CrC_{14}H_7O_9N_2$	398.21	Dark yellow	193	42.21 (42.88)	2.96 (3.03)	8.89 (9.02)
$[Mo(CO)_4L]$	$MoC_{14}H_7O_9N_2$	444	Yellow	181	39.55 (38.97)	2.72 (3.5)	8.13 (9.05)
$[W(CO)_4L]$	$WC_{14}H_7O_9N_2$	532.1	Orange	190	31.74 (32.08)	2.31 (2.9)	7.00 (8.02)

2.4.1 Materials and Reagents

Mammalian cell lines: breast cancer cell line (MCF-7), liver cancer cell line (HepG-2) and colon cancer cell line (HCT-116) were gained from Tissue Culture Unit (VACSERA) in El-Azhar University. DMSO solvent, trypan blue and crystal violet dye were obtained from Sigma (USA). DMEM, Fetal Bovine serum, L-glutamine, 0.25% Trypsin-EDTA, gentamycin, RPMI-1640, and (HEPES) buffer were obtained from Lonza. Crystal violet stain (1%) consisted of crystal violet 0.5% (w/v) and methanol 50% then made up to volume by ddH_2O and filtered through a Whatmann filter paper No.1.

2.4.2 Cytotoxicity estimation by viability assay

For the cytotoxicity assay, the tested cells were cultivated in a clean and dry 96-well plate at a cell concentration about 1×10^4 cells for each well in a growth medium of 100 µL. After 24 h of cultivation a fresh medium including distinct concentrations of the sample under investigation was inserted. Serial

doubled dilutions of the sample under investigation were added to cell mono layers distributed into 96-well, flat micro titer plates by a multichannel pipette. The micro titer plates were reserved at 37 ºC in a dampened incubator with 5% carbon dioxide for two days. For each sample concentration three wells were utilized. The control cells were incubated without the sample under investigation and with or without dimethyl sulfoxide solvent. After the cells incubation at 37 °C, several sample concentrations were inserted, then the incubation was preceded to additional 24 h and the yield of the viable cells was estimated using MTT assay [30, 31].Text graphics may be embedded in the text at the appropriate position.

3. Results and Discussion

3.1. Elemental analyses and physical properties

Both of the elemental analyses and physical properties of the free ligand and its corresponding metal carbonyl chelates are presented in Table (1).

Table (1): Properties of PNMA and its novel metal carbonyl mixed ligand chelates of ratio (1:1).

The resulted analytical data emphasize the suggested general formulae $[M(CO)_4L]$ of the newly synthesized chelates.

3.2. FT-IR spectroscopy

FT-IR results of PNMA ligand and its chelates are presented in Figures (1-4) and they are compared in Table (2).

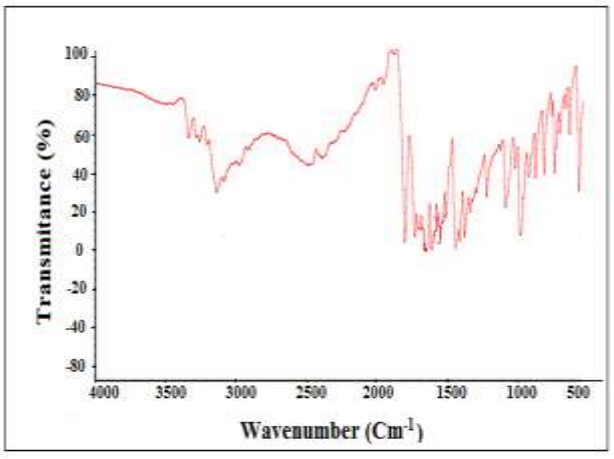

Fig. 1: FT-IR of *p*-nitrophenyl maleanilic acid ligand (PNMA)

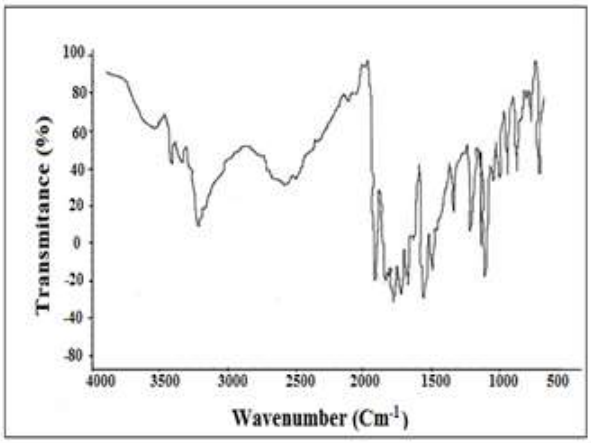

Fig. 2: FTIR of $[Cr(CO)_4L]$ complex.

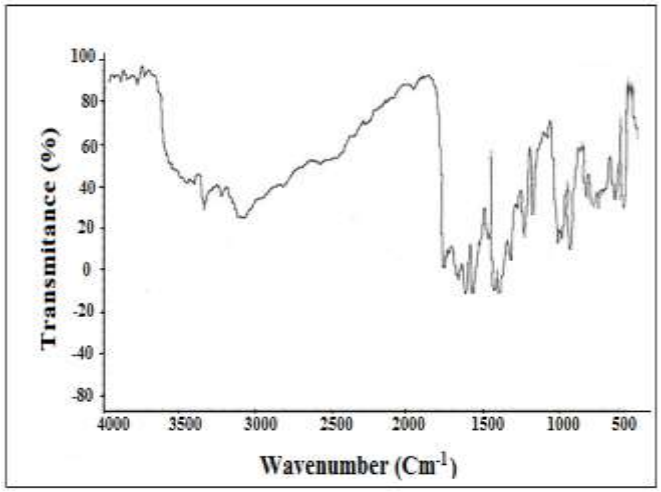

Fig. 3: FTIR of $[Mo(CO)_4L]$ complex.

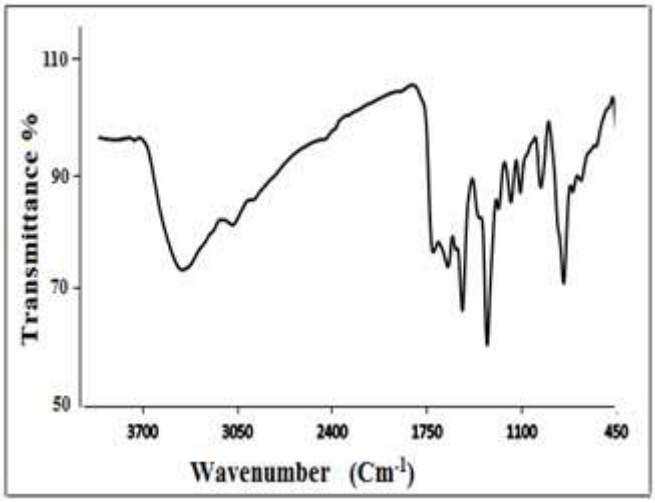

Fig. 4: FTIR of $[W(CO)_4L]$ complex.

Some data of selected characteristic functional groups of the free ligand and its novel chelates coming from the above figure are presented in Table (2).

Table (2): FT-IR data of PNMA ligand and its metal carbonyls complexes

Compound	υ(C=O) COOH cm^{-1}	υ(C=O) amide(I) (N-C=O) cm^{-1}	υ(O-H) cm^{-1}	υ(NH) amide cm^{-1}	υ(C=O) carbonyl cm^{-1}	υ(M-O) cm^{-1}	υ(M-C) cm^{-1}	υ (NO_2) cm^{-1}
L = PNMA	1706 s	1635 m	3292 s	3212 m	_____	_____	____	1512 st.as
$[Cr(CO)_4L]$	1705 s	1629 m	3401	3436 w	2062-1912-1875	503	549 m	1506 st,as
$[Mo(CO)_4L]$	1703 s	1607 m	3432	3401 w	2050-1975-1850	500	410 m	1503 st,as
$[W(CO)_4L]$	1706 s	1608 m	3418	3430 w	2285-1915-1840	584	469 w	1507 st,as

In KBr discs, band property: (s) strong, (m) medium, (w) weak, (as) asymmetric.

According to the free ligand FT-IR spectra and the data in Table (2); a broad band at 3292 cm^{-1} may imputed to the free ligand carboxylic group υ(OH) [32]. This band is shifted to (3401, 3432 and 3418) cm^{-1} in its chelates spectra. The υ(C=O) stretching band of free ligand carboxylic group observed at 1706 cm^{-1}, and the υ(C-O) stretching band appeared at 1306 cm^{-1} [32] and shifted to 1261, 1223 and 1257 cm^{-1} in FT-IR spectra of chromium, molybdenum and tungsten complexes respectively. These results indicating the participation of the carbonyl oxygen atom of the carboxylic group in coordination process between the free ligand and the metal carbonyls [33-35]. The free ligand showed a weak band at 3212 cm^{-1}; which may attributed to υ(N-H) amide group. This band moved to a higher frequency (3401-3436 cm^{-1}) in the metal complexes spectra. This shift indicated to the coordination process by the amide group nitrogen atom [34]. The metal carbonyl complexes spectra offer three stretching bands. The first stretching band observed at (2075, 2050 and 2285) cm^{-1} for $[Cr(CO)_4L]$, $[Mo(CO)_4L]$ and $[W(CO)_4L]$ respectively. This band may attribute to the two carbonyl groups in Trans position. The other two carbonyl groups observed as symmetrical and asymmetrical stretching bands at (1875, 1850 and 1840) cm^{-1} and (1912, 1950 and 1914) cm^{-1} for $[Cr(CO)_4L]$, $[Mo(CO)_4L]$ and $[W(CO)_4L]$ respectively [36, 37]. FT-IR spectra of the metal carbonyl chelates exhibit a stretching frequency bands at (503, 500 and 584) and (549, 410 and 469) cm^{-1}. These bands may related to υ(M-O) and υ(M-CO), in addition to the bands which may referred to υ(M-N) [36, 38].

The resulted FT-IR data for (L) ligand and its metal carbonyl complexes prove that; the suggested structure of the novel chelates may be as assigned as in Figure (5).

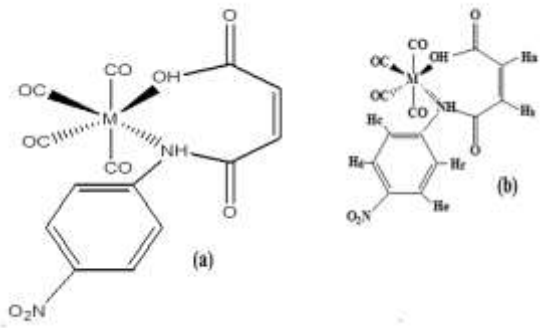

Fig. (5): The predicted structure of the novel complexes [M = Cr, Mo or W].

3.3. ^{1}H-NMR measurements

The ^{1}H-NMR spectra of PNMA ligand and its metal carbonyls complexes of the type $[M(CO)_4L]$, (M = Cr, Mo or W and L = PNMA = *p*-nitrophenyl maleanilic acid) are studied and investigated. The results are tabulated in Table (3).

a-In DMSO, chemical shifts, δ, to high frequency of TMS.

The ^{1}H-NMR spectrum of PNMA free ligand shows two singlets. The first singlet of relative intensity 1H observed at δ 12.98 ppm and it may assign to OH proton of the carboxylic acid. This singlet is moved to δ 12.12 and δ 11.047 ppm in spectra of

$[Mo(CO)_4L]$ and $[W(CO)_4L]$ respectively, this indicate to the possibility of sharing the carboxylic group in the coordination with the metal atoms. The second singlet of relative intensity 1H appeared at δ 10.84 ppm and may imputed to the amide proton HNCO. This signal is slightly shifted to δ 11.04 ppm in spectra of Mo(0) and W(0) complexes, this shift may attribute to the possibility of amide group participation in the coordination process. The ^{1}H-NMR of PNMA ligand and its complexes show distinguished doublets of the aromatic protons ortho to nitro group (H^e, H^d). Doublets of free ligand are a little shifted to δ 7.89-7.83 ppm and δ 7.17-6.74 ppm for Mo(0) and W(0) complexes respectively. The other doublets manifested at δ 8.23-8.20 ppm for the ligand aromatic protons ortho to amide group (H^c, H^f) are slightly shifted to δ 7.86-7.80 ppm and δ 7.14-6.71 ppm for Mo(0) and W(0) complexes respectively. These signals pointed to the existence of four protons of two couples; which they are only chemically not magnetically equivalent [39]. The free ligand vinylic proton H^a observed as doublets at δ 6.34-6.36 ppm and it is noticed slightly shifted to δ 6.70-7.13 ppm and δ 6.70-6.73 ppm for Mo and W complexes respectively. The other vinylic proton H^b; which resonates at δ 6.32-6.35 ppm is shifted to δ 6.74-7.17 ppm and δ 6.72-6.75 ppm for Mo and W complexes respectively. Finally, eight lines were observed consistent with the pattern expected for an **AA' XX'** spin system [40] J_{AX} and $J_{AX'}$ were calculated in Table (3). These shifts are confirming the tolerance of chelation between the ligand and the metal carbonyls through the carboxylic and amide groups of the free ligand (Figure 5b).

3.4. Mass spectra of ligand chelates

The mass spectra of $[Cr(CO)_4L]$ present the main molecular ion and many fragment ions are presented in Figure (6).

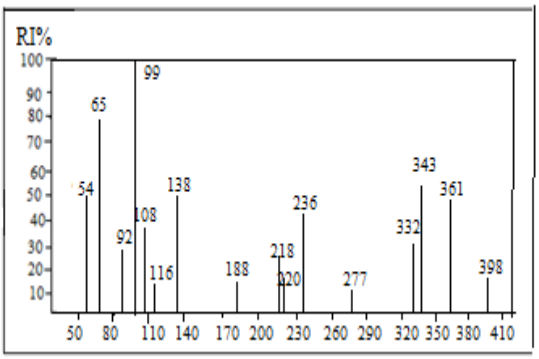

Fig. (6): Mass Spectra of $[Cr(CO)_4L]$ complex.

The major fragmentation pathways of $[Cr(CO)_4L]$ chelate show the major molecular ion $[C_{14}H_6N_2O_9Cr]^+$ of m/z = 398 (RI = 19 %) as represented by Scheme (3). The low relative intensity of the main molecular ion of $[Cr(CO)_4L]$ at 70 eV may be attributed to its gaining of high energy which leads to its parallel fragmentation pathways.

The proposed fragmentation of $[Cr(CO)_4L]$ reveals three fragmentation pathways that can be rationalized in Scheme (3). Path way I reveals the signal of the fragment ion $C_8H_3O_7NCr^+$ at m/z = 277 by the rupture of 4-nitrobenzene from the entity of the molecular ion. The fragment ion at m/z = 221 (mole mass = 221, RI = 14 %) may assigned to the loss of two CO groups. This is followed by the fragment ion at m/z = 108; which may indicated to the loss of 4-amino-4-oxobut-2-enoic acid. The second path way presents fragment ions at m/z = 343, 235 and 116 (mole mass = 343, 236 and 114 with RI = 55, 45 and 10 %). These signals may imputed to the rupture of 2CO groups from the molecular ion followed by $Cr(CO)_2$ loss, then the loss of 4-nitrobenzene. Path way III shows that the molecular ion loosed $Cr(CO)_2$ at first with a signal at m/z = 235 (mole mass = 236, RI = 45 %) followed by the loss of 4-nitrobenze.

Table (3): ^{1}H-NMR data for PNMA ligand and its metal chelates of the type $[M(CO)_4L]$.

Compound	δO-H	δN-H	δH^a	δH^b	δH^c	δH^d	δH^e	δH^f	$^3J(H^a\text{-}H^b)$	$^3J(H^c\text{-}H^d)$	$^3J(H^e\text{-}H^f)$
L = PNMA	12.98	10.84	6.34	6.32	8.23	7.93	7.93	8.23	5.7	6.6	12.3
			6.36	6.35	8.20	7.88	7.88	8.20			
$Mo(CO)_4L$	12.12	10.62	6.70	6.74	7.86	7.89	7.89	7.86	12	9	9
			7.13	7.17	7.80	7.83	7.83	7.80			
$W(CO)_4L$	11.05	10.61	6.70	6.72	7.14	7.17	7.17	7.14	6	9	9
			6.73	6.75	6.71	6.74	6.74	6.71			

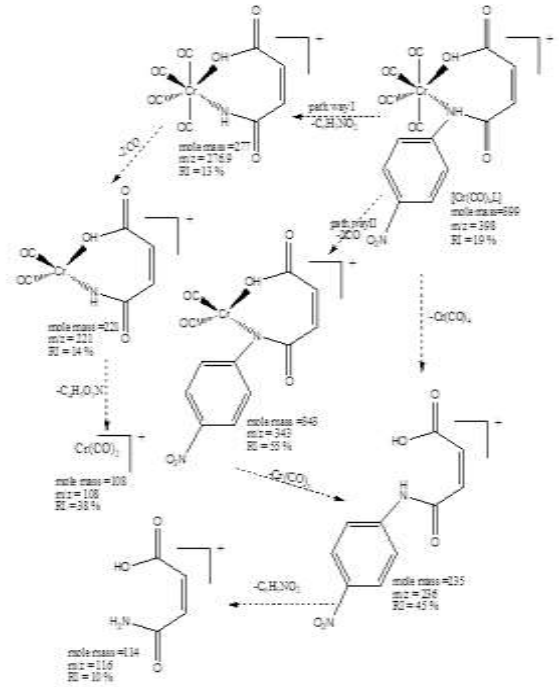

Scheme 3: The pathways mass fragmentation of $[Cr(CO)_4L]$

The mass spectrum of $[Mo(CO)_4L]$ chelate at 70 eV is presented in Figure (7).

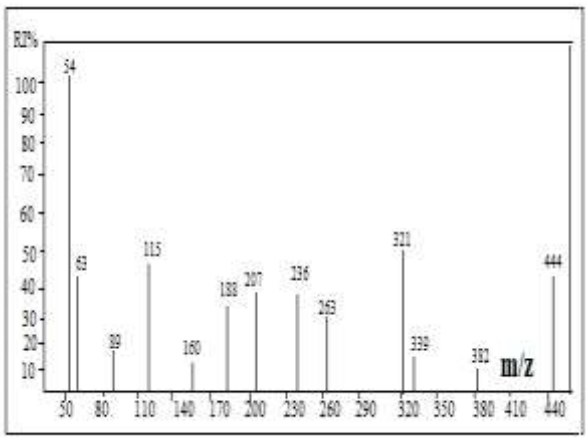

Fig. (7): Mass Spectra of $[Mo(CO)_4L]$ complex

EI-MS of $[Mo(CO)_4L]$ complex presents the formation of many fragment ions; which are given in Scheme (4). The signal manifested at m/z = 444 (RI = 42 %) may imputed to the molecular ion.

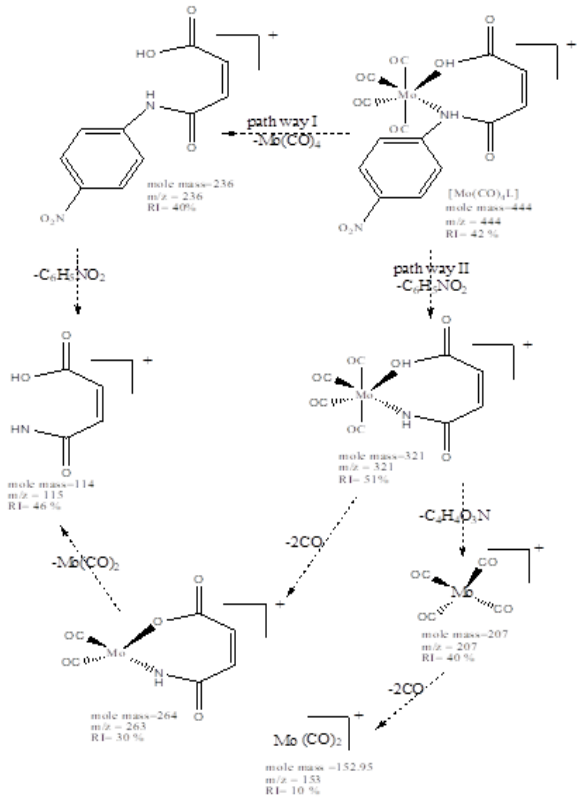

Scheme 4: The mass fragmentation pathways of $[Mo(CO)_4L]$.

The mass fragmentation pathways of $[Mo(CO)_4L]$ complex are floated in Scheme (4) in two parallel pathways. The first path way shows two fragment ions appeared at m/z = 236 and 115 (mole mass = 236 and 114, RI = 40 and 46 %); which may referred to the liberated of $Mo(CO)_4$ from the parent ion followed by the loss of 4-nitrobenzene. The second path way gives a signal at m/z = 321 (mole mass = 321, RI = 51 %); which may imputed to the rupture of 4-nitrobenzene. This fragment can be rupture through two different bond positions, firstly it can loosed 4-amino-4-oxobut-2-enoic acid and give signal at m/z = 207 (RI = 48 %); then the liberation of pair of CO molecules (m/z = 153, RI = 10 %).The second possible position through the liberation of two CO gas molecules and give a signal at m/z = 263, RI = 30 %; followed by the liberation of $Mo(CO)_2$ (m/z = 115, RI = 46 %).

Mass spectrum of $[W(CO)_4L]$ complex at 70 eV is shown in Figure (8).

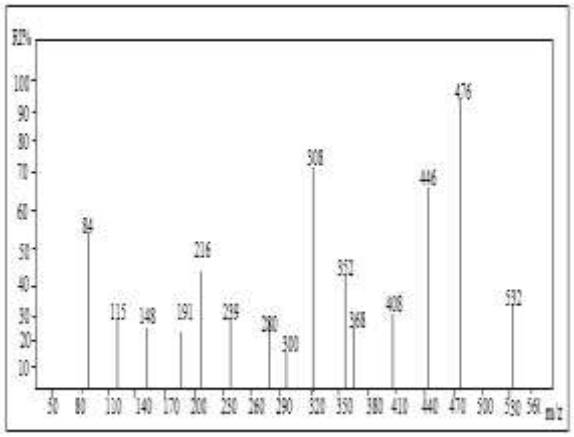

Fig. (8): Mass Spectrum of $[W(CO)_4L]$ complex. The main fragments were obtained and identified in Scheme (5).

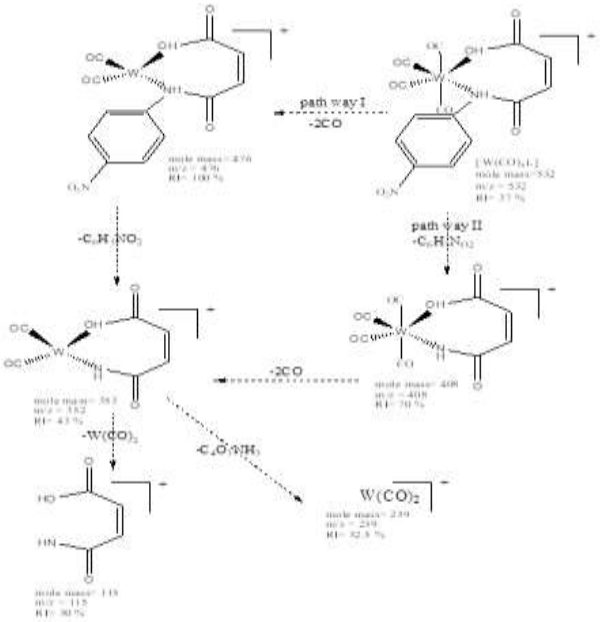

Scheme 5: The mass fragmentation pathways of the principle fragmentations of $[W(CO)_4L]$.

Mass spectra of $[W(CO)_4L]$ complex present the main molecular ion at m/z = 532. Scheme (5) shows two possible parallel pathways of the fragmentation. The base peak at m/z = 476 (mole mass = 476, RI = 100 %) in pathway I may refers to the loss of two carbonyl groups as two CO gas molecules from the entity of the molecular ion followed by the fragment ion at m/z = 352 (mole mass = 353, RI = 43 %) due to the breakage of $C_6H_6NO_2$. The signal appears at m/z = 115 (mole mass = 115, RI = 30 %) may attribute to the breakage of W $(CO)_4$. Pathway II (Scheme 5) shows a peak at m/z = 408 (mole masses = 408, RI = 70 %); which may imputed to the cleavage of $C_6H_6NO_2$ from the entity of the molecular ion. There is a signal appears at m/z = 352 (mole mass = 353, RI = 43 %) may refer to the loss of two carbonyl groups as two molecules of CO gas. Then the appearance of a signal at m/z = 115 (mole mass =115, RI = 30 %); may assigned to the break of (Z)-4-amino-4-oxobut-2-enoic acid.

3.5 Thermal Analyses (TA)

TGA curves of the prepared compounds are shown in Figures (9a, 9b, 9c), and the data are sorted in Table (4).

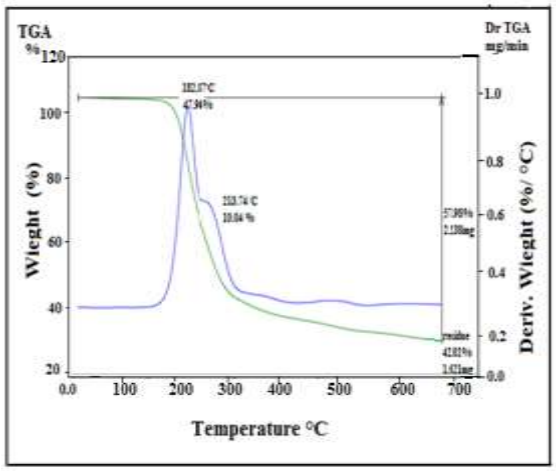

Fig.(9a): TGA and DTG curve of $[Cr(CO)_4L]$

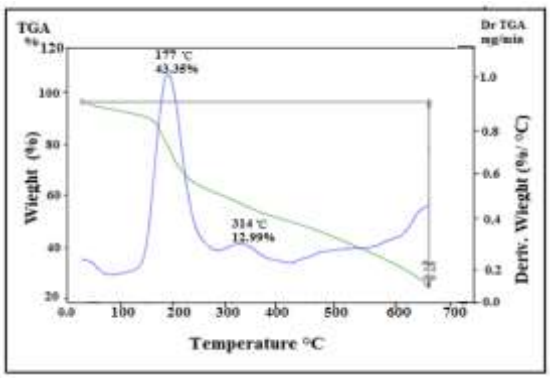

Fig.(9b): TGA and DTG curve of $[Mo(CO)_4L]$

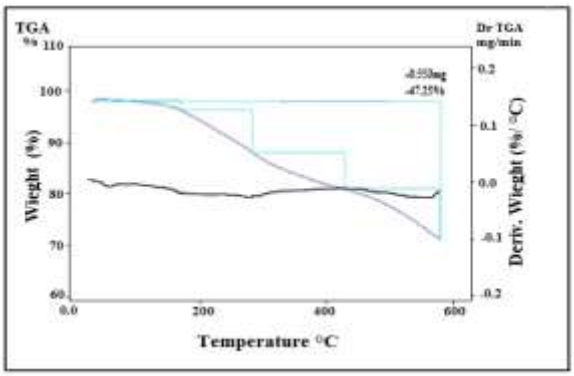

Fig.(9c): TGA and DTG curve of $[W(CO)_4L]$

Table (4): Data of thermal analyses of the newly synthesized complexes.

Compound	TGA temp. range (°C)	DTG temp (°C)	Mass loss (calcd.) %	TGA description
[$Cr(CO)_4L$]	150-190	182.87	47.94 (49.80)	-The loss of PNMA ligand
	191-240	213.74	10.04 (11.86)	-The loss of 2CO groups
[$Mo(CO)_4L$]	120-190	177.33	43.35 (45.82)	-The loss of PNMA ligand
	190-340	314.34	12.99 (12.64)	-The loss of 2CO groups
[$W(CO)_4L$]	182.7-299.1	201.2	37.86 (38.8)	-The loss of PNMA ligand
	299.1-445.6	300.8	4.66 (4.62)	-The loss of CO group
	445.6-598	459	4.73 (4.62)	-The loss of CO group

The thermodynamic activation parameters of the metal chelates decomposition processes included activation energy (E*), entropy (ΔS*), enthalpy (ΔH*) and Gibb's free energy change (ΔG*) are calculated from TGA and DTGA data and they are tabulated in Table (5) using Coats-Redfern equation [41].

According to the TGA data of [$Mo(CO)_4L$] complex, the thermal decomposition of this complex happened through two essential steps. The initial one began at 120 °C and it extended to 190 °C with evaluated mass loss of 43.35 % (calcd. 45.55 %) and DTG peak at 177.33 °C. This peak may attribute to the separation of the free ligand (L) from the entity of complex. The other decomposition step occurred through the

Table (5): Activation thermodynamic parameters of the metal chelates

Compound	Step	Temperature range (°C)	E^* kJ.mol^{-1}	A S^{-1}	ΔS^* $JK^{-1}mol^{-1}$	ΔH^* kJ.mol^{-1}	ΔG^* kJ.mol^{-1}
[$Cr(CO)_4L$]	1	150-190	259.698	3.99439E+29	-226.81	255.905	359.302
	2	191-240	152.713	5.20582E+15	-231.77	148.664	261.476
[$Mo(CO)_4L$]	1	120-190	96.125	40080013025	-234.97	92.3785	198.194
	2	190-340	41.679	3228413.259	-244.13	36.796	180.097
[$W(CO)_4$ L]	1	182.7-298	69.6	8.896E+05	-134.90	65.6	129.6
	2	299.1-445.6	71.35	1.600E+05	-150.75	66.58	153.08
	3	445.6-598.	152.55	5.552E+08	-84.993	146.46	208.67

The TGA results refer to the decomposition of [$Cr(CO)_4L$] complex took place in two main steps. The first step occurred in temperature range 150-182 °C, DTG peak at 182.87 °C and the estimated mass loss of 47.94 (calcd. 49.80 %). This peak may attribute to the removal of PNMA ligand from the moiety of the complex. The other step took place within the temperature range 182-213 °C, DTG peak at 213.74 °C and with estimated loss of 10.04 % (calcd. 11.86 %). This step may attribute to the separation of two CO groups from the entity of the complex. These steps of decomposition required activation energy values of 259.698 and 152.713 kJ.mol^{-1} respectively. ΔS^* negative values (-226.81 and -231.77 J K^{-1} mol^{-1}) may assigned to the constancy of the released fragments. Values of obtained thermodynamic parameters of [$Cr(CO)_4L$] complex are given in Table (5). The practical mass loss is about 57.98 % (calcd. 61.66 %) and the residual product may be $Cr(CO)_2$ of practical mass 42.02 % (calcd. 38.34 %).

temperature range 190-340 °C and DTG peak at 314.34 °C with evaluated mass loss of 12.99 % (calcd. 12.64 %). This step may relate to the separation of 2CO groups from the skeleton of the complex. These mass losses observed as two endothermic peaks at 165 and 496 °C respectively. These endothermic peaks followed by two exothermic peaks; which may assigned to the chemical rearrangement of the fragments during the decomposition. These mass losses required energy values of 259.698 and 152.713 kJ. mol^{-1} respectively. The ΔS^* negative values (-234.97 and -244.13 J K^{-1} mol^{-1}) may refer to the steadiness of the liberal fragments. The obtained values of thermodynamic parameters of [$Mo(CO)_4L$] complex are presented in Table (5). The total mass loss = 56.34 % (calcd. 58 %) and the remainder was proposed as $Mo(CO)_2$ of the practical mass of 43.66 % (calcd. 42.6 %).

Thermal decomposition of [$W(CO)_4L$] metal complex took place in three sequential steps. The first step happened at the temperature range 182-298 °C of evaluated mass loss of 38.8 % (calcd. 37.86 %). First step involved the loss of PNMA ligand molecule from the moiety of complex and the maximum rate of

mass loss is obtained by DTG curve at 201.20 °C. The other step took place in the temperature range 298-446 °C and DTG peak at 300.80 °C, in which CO group is separated with mass loss of 4.62 % (calcd. 4.66 %). The last step began at 446 °C and continued to 598 °C and the peak of DTG occurred exactly at 459 °C with estimated mass loss = 4.62 % (calcd. 4.73 %). This step corresponded to the breaking of another CO group. The observed overall mass loss = 47.25 %; which it is in a good harmonization with the theoretical estimated value of 47.04 %. The remainder end product may be $W(CO)_2$. The practical and the theoretical data are presented in Table (5). The thermodynamic parameters obtained from TG and DTG data of $[W(CO)_4L]$ are calculated and presented in Table (5). The obtained ΔS^* negative values of 134.9, 150.75 and 84.99 J K^{-1} mol^{-1} may impute to the distinction of disorder degree of the system during the diverse steps of weight losses. The descending of ΔS^* negative values may refer to the increasing of disorder through the decomposition steps of $[W(CO)_4L]$ metal complex.

3.6. The correlation of the mass spectra and the thermal analyses of the novel complexes

3.6.1. $[Cr(CO)_4L]$ chelate

EI-MS data of $[Cr(CO)_4L]$ is presented in Figure (6) and the possible pathways are shown in Scheme (3). The first pathway of the cleavage started with the formation of the fragment ion $C_8H_3O_7NCr^+$ at m/z = 277 due to the rupture of 4-nitrobenzene from the entity of molecular ion. This step followed by the observation of fragment ion at m/z = 221 (mole mass = 221, RI = 14 %); which may imputed to the liberation of 2CO molecules. The resulted fragment from the above step loosed 4-amino-4-oxobut-2-enoic acid and the final residual product may be $Cr(CO)_2$. This conclusion is rationalized by the TGA and DTG analyses; in which the complex thermally decomposed through two steps at temperature ranges 150-182 and 182-213 °C respectively. The metal chelate loosed PNMA ligand at the first step then it loosed two CO gas molecules. The residual product was as the same as those of EI-MS with actual mass of 42.02 % (calcd. 38.34 %).

3.6.2. $[Mo(CO)_4L]$ complex

Mass spectrum of $[Mo(CO)_4L]$ offers several fragmentation pathways as shown in Scheme (4). The second pathway presents a signal at m/z = 444, RI = 42 % may assigned to the molecular ion fragment; which it started to loose *p*-nitrobenzene and give $C_8H_3O_7NMo$ fragment ion of m/z = 321, RI = 51 %. This followed by the observation of $Mo(CO)_4^+$ fragment ion (m/z = 207, RI = 40 %); which it may attributed to the loss of 4-amino-4-oxobut-2-enoic acid. Finally the liberation of two molecules of CO gas from the above fragment and the remainder product may be $Mo(CO)_2$ (m/z = 153, RI = 18 %). This conclusion is in agreement with the TGA and DTG results; which show the thermal decomposition of the metal chelate through two main steps. The first one began at 120 °C and extended to 177 °C, DTG peak at 177.33 °C with evaluated mass loss of 43.35 % (calcd. 45.55 %). This peak may imputed to the cleavage of PNMA ligand; while the other step occurred in the temperature range from 177 °C to 314 °C and the DTG peak observed at 314.34 °C with evaluated mass loss of 12.99 % (calcd. 12.64 %). This step may impute to the liberation of two CO molecules. The overall mass loss was 56.34 % (calcd. 58 %) and the final residual product was as the same as that shown in EI-MS with actual mass of 43.66 % (calcd. 42.6 %).

3.6.3. $[W(CO)_4L]$ complex

The mass spectra of $[W(CO)_4L]$ (Figure 8) show the possible fragmentation pathways (Scheme 5); in which the main molecular ion observed at m/z = 532, RI = 37 %. Pathway II presented a peak at m/z = 408 (mole masses = 408, RI = 70 %), this peak may assigned to the cleavage of $C_6H_6NO_2$ from the entity of the molecular ion. Another signal appeared at m/z = 352 (mole mass = 353, RI = 43 %); which may referred to the loss of two molecules of CO and the signal appeared at m/z = 115 (mole mass =115, RI = 30 %) may imputed to the cleavage of (Z)-4-amino-4-oxobut-2-enoic acid. As mention before in TGA and DTG data of $[W(CO)_4L]$ resulted in this complex is thermally decomposed in three sequential steps. The first one occurred in temperature range 182-298 °C; in which 4-nitrophenyl maleanilic acid ligand is decomposed. Secondly, at the temperature range of 298-446 °C one molecule of CO gas liberated from the entity of the complex, followed by removal of a another CO gas molecule in temperature range from 446 to 598 °C. The remainder end product may be $W(CO)_2$ this remainder part appeared in mass at m/z = 239 (RI = 32.5 %). According to the EI-MS results of $[W(CO)_4L]$ complex, the conclusion is both the EI-MS data and thermal analyses of the complex are in harmony with each other.

3.7 X-ray powder diffraction (XRD)

The XRD pattern of PNMA ligand and its metal carbonyl mixed ligand complexes is presented in Figure (10).

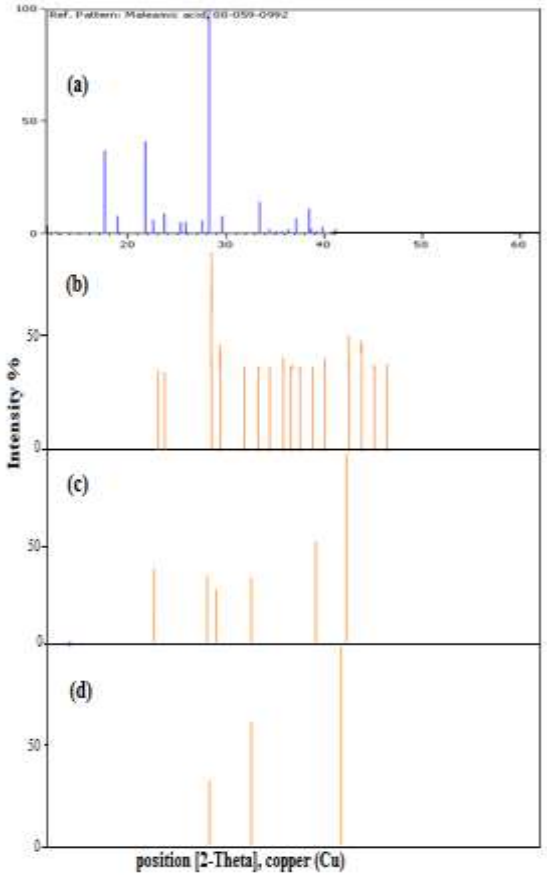

Fig. (10): X-ray diffraction peak list of (a) PNMA free ligand, (b) Cr(0), (c) Mo(0) and (d) W(0) complexes.

Comparing the XRD spectrum of PNMA free ligand with that previously published [42], patterns with matching peaks are obtained pointing the presence of the free ligand molecule in a monoclinic form. The XRD data for complexes show that, the chelation of the free ligand to the Chromium, Molybdenum, and Tungsten changed the XRD pattern of the free ligand. This indicates that the synthesized complexes are not fitted in the same phase of free ligand. Subsequently, the non-similarity of the free ligand XRD pattern and its metal carbonyl complexes propose that these complexes have a distinct phase structure than the PNMA free ligand. The appearance of various lines at different 2Ɵ values in XRD of distinct chelates may refer to different shapes of these chelates as confirmed by different mass and TGA fragmentation pathways. The variation of peaks of PNMA complexes may related to differences in modes of chelation of the ligand to the corresponding metals (Cr, Mo, and W) as given in their forms (Figure 5).

3.8 Anticancer Activity

Cytotoxic activity of PNMA free ligand and its chromium complex versus three human cancer cell lines included MCF-7 (breast cancer cell), HCT-116 (colon cancer cell), and finally HepG-2 (liver cancer cell). These cells are estimated by viability assay [43], as shown in Figures (11, 12). The concentrations of them ranged from 3.9 to 500 µg mL^{-1}.

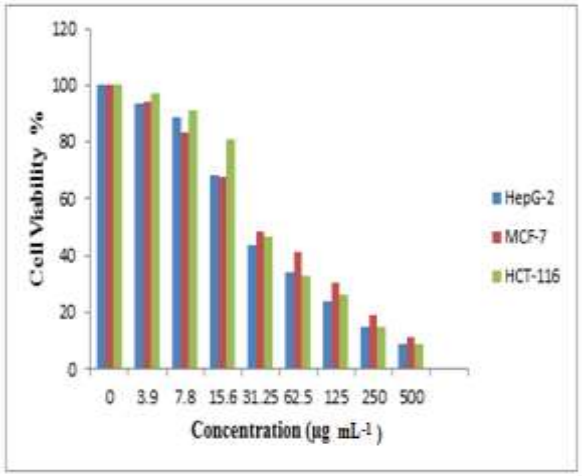

Fig. (11): Cell viability of PNMA versus three tested human cell lines

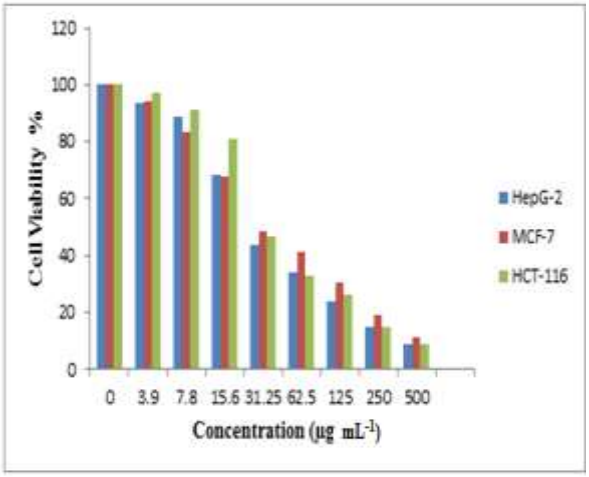

Fig. (12): Cell viability of $[Cr(CO)_4L]$ complex versus three tested human cell lines.

Cytotoxicity in vitro of PNMA ligand and its chromium complex are estimated by MTT assay against three typical human tumor cell lines involving HCT-116, MCF-7, and finally HepG-2 cell lines. The obtained curves are presented in Figures (11, 12) and the results are scheduled in Table (6).

Table (6): Influence of PNMA ligand and its chromium complex on the viability of HCT-116, MCF-7, and HepG-2 cells

Compound	Cytotoxicity in vitro IC_{50} (µg mL^{-1})		
	HepG-2	MCF-7	HCT-116
***p*-nitrophenyl maleanilic acid (L = PNMA)**	15.1	25.9	26.7
$[Cr(CO)_4L]$	27.3	30.1	29.6

Figure (11) illustrates the inhibitory rate of PNMA free ligand and it is remarkable, the free ligand exhibited high cytotoxicity against the selected human cancer cells. Also it shows the highest inhibitory influence against HepG-2 with IC_{50} = 15.1 µg mL^{-1} than MCF-7 of IC_{50} = 25.9 µg mL^{-1} and HCT-116 of IC_{50} = 26.7 µg mL^{-1}. Treatment of HCT-116, HepG-2, and MCF-7 cell line with $[Cr(CO)_4L]$ complex led to a significant decrease in the cell viability of the three human tested cell lines with increasing the concentration of it, as shown in Figure (12). The IC_{50} values are 30.1, 27.3 and 29.6 µg mL^{-1} for the hepatocellular, the breast, and the colon cancer cell lines respectively, these values of IC_{50} of $[Cr(CO)_4L]$ complex are slightly less than that of the corresponding PNMA free ligand, as presented in Table (6). IC_{50} values were evaluated according to the curves of the respective dose response and are abstracted in Table (6). The results of the MTT assay of $[Cr(CO)_4L]$ complex clarified that the free ligand inhibitory potency was slightly decreased by the complexation with $Cr(CO)_6$. These results were explained in the same way like that previously published [44-46] in research our group.

4. Conclusion

The ligand (PNMA) had been synthesized and characterized. Also novel tetra carbonyl *p*-nitrophenyl maleanilic acid organometallic complexes of Cr, Mo and W metal atoms are successfully synthesized and structurally characterized. These complexes are confirmed to have 1:1 (L: M) stoichiometric ratio and they have been found they are mononuclear complexes. The structure of both of PNMA free ligand and its identical novel complexes are characterized by distinct tools involved elemental analyses, spectroscopic measurements (FT-IR, ^{1}H-NMR, and EI-MS) and they are supported by thermal analyses. Also from the XRD data it was cleared that the novel metal complexes of PNMA ligand have structures as revealed by sharp lines that differ from those of the free ligand itself. The anticancer efficacy of PNMA ligand and its novel chromium complex are examined. PNMA ligand presents slightly higher inhibitory efficacy than those of its chromium complex against the detected cancer cell lines under investigation (HCT-116, MCF-7, and HepG-2 cell lines).

.

Acknowledgments

The authors recognize the upholding of this study given by the Chemistry Department at both Aswan University and Cairo University.

Authors declare that there is no conflict of interest

References

[1] Pearson R.G., S. *Chem. Ed*., 45, 581(1968).

[2] Cotton F. A., Proposed nomenclature for olefin-metal and other organometallic complexes. *Journal of the American Chemical Society*. 90, S, 6230–6232 (1968)

[3] Dyson P. J., McIndoe J. S., Transition Metal Carbonyl Cluster Chemistry. *Amsterdam: Gordon & Breach (*2000).

[4] a) Huheey J. E., Inorganic Chemistry: Principle of Structure and Reactivity, 4th ed.; Harper Collins College Publishers: New York (1993). b) Cotton F. A., Wilkinson G., Advanced Inorganic Chemistry, 4th ed.; Wiley: New York (1980).

[5] Elschenbroich C., Salzer A., Organometallics, 2nd ed.; VCH: Weinheim, Germany (1992).

[6] Dewar M. J., *Bull. Soc. Chim.* Fr., 18, C79 (1951).

[7] Chatt J., Duncanson L. A., *J. Chem. Soc*., 2929 (1953).

[8] a) Hoffmann R., Chen M. M. L., Thorn D. L., *Inorg. Chem*., 16, 503 (1977). (b) Schilling B. E. R., Hoffmann R., *J. Am. Chem. Soc*., 101, 3456 (1979). (c) Hoffmann R., *Science*, 211, 995 (1981). (d) Hoffmann R., Albright T. A., Thorn D. L., *Pure Appl. Chem*., 50, 1 (1978).

[9] Albright T. A., Burdett J. K., Whangbo M. H., Orbital Interactions in Chemistry; Wiley: New York, (1985).

[10] Werner H., Angew G. A. *Chem., Int. Ed. Engl*., 29, 1077 (1990).

[11] (a) Ellis J. E., *Adv. Organomet. Chem*., 31, 1 (1990). (b) Kundig E. P., Moskovits M., Ozin G. A., Angew. Chem. 1975, 87, 314; *Angew. Chem., Int. Ed. Engl*., 14, 292 (1975). (c) Ozin G. A., *Acc. Chem. Res*., 10, 21(1977).

[12] Hurlburt P. K., Rack J. J., Luck J. S., Dec S. F., Webb J. D., Anderson O. P., Strauss S. H., *J. Am. Chem. Soc.*, 116, 10003 (1994).

[13] Elschenbroich C., Organometallics. Weinheim: Wiley-VCH, (2006).

[14] Hanford W. E., Fuller D. L., *Industrial & Engineering Chemistry*, 40 (7), 1171-1177 (1948).

[15] Sargent A. L., Hall M. B., "Linear Semibridging Carbonyls. 2. Heterobimetallic Complexes Containing a Coordinatively Unsaturated Late Transition Metal Center". *Journal of the American Chemical Society*, 111 (5): 1563–1569(1989).

[16] Cava M. P., Deana A. A., Muth K., Mitchell M. J., N-phenylmaleimide, Organic Syntheses, 41, 93(1961).

[17] Harrison A. G., Kallury R. K. M., Stereo chemical applications of mass spectrometry. II—Chemical ionization mass spectra of isomeric dicarboxylic acids and derivatives, *Organic Mass Spectrometry*, 15, 277(1980).

[18] Corrie J. E. T. J., Thiol-reactive fluorescent probes for protein labeling. *Chem. Soc. Perkin Trans*, I., 2975-2982(1994).

[19] Shahid K., Ali S., Shahzadi S., Badshah A., Khan K., Maharvi G. M., Organotin (IV) Complexes of Aniline Derivatives.I. Synthesis, Spectral, and Antibacterial Studies of Di-and Triorganotin (IV) Derivatives of 4-Bromomaleanilic Acid, Synthesis and reactivity in inorganic and metal-Organic chemistry., 33, 7, 1221–1235(2003).

[20] Islam M. S., Hossain M. B. D., Reza M. Y., antimicrobial study of mixed ligand transition metal complexes of maliec acid and heterocyclic amine bases., *J.Med.Sci*., 3(4), 289-293(2003).

[21] IUPAC Publisher," A Guide of IUPAC Nomenclature of Organic Compounds", P-65.1.6, Blackwell Scientific Publication, IUPAC, (1993).

[22] Ravindar V., Lingaiah P., Effect of Amide Group Ligands and their Metal Complexes on Pathogenic Fungi. *Current science*, 53, 19(1984).

[23] Anand P., Singh B., Synthesis and evaluation of novel 4-[(3H,3aH,6aH)-3- phenyl)-4,6-dioxo-2-phenyldihydro-2H-pyrrolo[3,4-d] isoxazol-5(3H,6H,6aH)- yl] benzoic acid derivatives as potent acetyl cholinesterase inhibitors and anti-amnestic agents., *Bio Org Med Chem*., 20 (1), 521(2012).

[24] Fujinami A., Ozaki T., Nodera K., Agric K., Studies on Biological Activity of Cyclic imide Compounds, Part II. Antimicrobial Activity of l-Phenylpyrrolidine-2, 5-diones and Related Compounds. *Biol. Chem*., 36, 318(1972).

[25] Rodolfo A., Valencia H., Pardo Z. D., Vriesa R., Kennedy A. R., *Acta Cryst*., 62، 2734(2006).

[26] Li Z. X., Ren C. M., Yang S., Yao G. Y., Shi Q. Z., (Z)-(2-Furyl) (2-naphthylamino) methylene)]-3- Methyl-1-phenyl-1H-pyrazol-5(4H)-one. Corrigendum. *Acta Cryst*., 65, 65(2009).

[27] Saedi H., Solvent free preparation of N-substituted maleanilic acid. *Chem. Soc. Ethiop*, 27(1), 137- 141(2013).

[28] Cooper G. R., Mcewan D. M., Shaw B. L., *Inorganica.Chimica.Acta*., 76, 165-166(1983).

[29] Cooper G. R., Hassan F., Shaw B. L., and Thorntonpett M. J., *Chem.Soc., Chem. Commun*, 614-616(1985).

[30] Mosmann T., Rapid colorimetric assay for cellular growth and survival: application to proliferation and Cytotoxicity assays. *J. Immunol. Methods*, 65: 55-63(1983).

[31] Gomha S. M., Riyadh S. M., Mahmmoud E. A., and Elaasser M. M., Synthesis and Anticancer Activities of thiazoles, 1, 3-Thiazines, and Thiazolidine Using Chitosan-Grafted-Poly (vinyl pyridine) as Basic Catalyst. *Heterocycles*, 91(6):1227-1243(2015).

[32] M. A. Zayed, M. El-desawy, A. A. Eladly, Egypt.J.Chem. 2019, 62, 8, 1519 – 1536.

[33] Pretsch E., Buhlman P., Badertscher M., structure determination of organic compounds, Fourth edition,(2008).

[34] Max J.J., Chapados C.," Infrared Spectroscopy of Aqueous Carboxylic Acids: Comparison between Different Acids and Their Salts". *The Journal of Physical Chemistry*, A 108, 16 (2004).

[35] Sandhu S. S., Manhas P. S., Mittal M. R. and Parmer S. S., *Indian J. Chem*, 7, 286(1969).

[36] Kaushik M., Singh A., and Kumar M., "The chemistry of group - VIb metal carbonyls". *European Journal of Chemistry*, 3, 3, 367- 394 (2012).

[37] Braterman P. S., "Metal Carbonyl Spectra". *Academic Press*, (1975).

[38] Jones L. H., A Resonance Interaction Valence Force Field for Octahedral M(XY), Molecules. Journal of Molecular Spectroscopy, 8, 195-129 (1962).

[39] Pringle P. G., Shaw B. L., *J Chem .Soc. Chem. Commun*., 581(1982).

[40] Silvertein, R.M; Bassler, G.C., Spectrometric Identification of Organic Compounds, John Wiley and Sons: New York, (1967).

[41] Coats A. W., Redfern J. P., *Nature, London*, 201, 68- 69(1968).

[42] Rafalska-Lasocha A., Jagiellonian Univ., Krakow, Poland ،*ICDD* Grant-in-Aid, (2007).

[43] Gomha S. M., Edrees M. M., Altalbawy F. M. A., Synthesis and Characterization of Some New Bis-Pyrazolyl-Thiazoles Incorporating the Thiophene Moiety as Potent Anti-Tumor Agents. *Int. J. Mol. Sci.*, 17, 1499(2016).

[44] Zayed M., Zayed M.A., Abd El Salam H. A., Noamaan, M. A. Novel Triazole Thiole ligand and some of its metal chelates: Synthesis, structure characterization, thermal behavior in comparison with computational calculations and biological activities, Computational Biology and Chemistry 78 (2019) 260–272.

[45] Zayed M. A., Abdallh M. A., Structure Investigation of Solid Ion Pairs of Three Imidazole Drugs-rose Bengal Using Different Spectroscopic Techniques and their Biological Activities, Egypt.J.Chem. Vol. 62, No. 11. pp. 2143 - 2162 (2019).

[46] Abd El Salam H.A., Zayed E. M., Zayed M. A., Noamaan, M. A. : Synthesis, Structural Characterization, Thermal Behavior and Antimicrobial Activity of Copper, Cadmium and Zinc Chelates of Traizole-thiole Ligand in Comparison with Theoretical Molecular Orbital Calculations, Egypt.J.Chem. Vol. 62, Special Issue (Part 1), pp. 145 - 163 (2019).

التحضير والتوصيف الفيزيائي والكيميائي و فعالية التسمم لحمض البارا نيترو فينيل مالينيليك و متراكباته

الكربونيلية ذات الليجاندات المختلطة

محمد عبد الجواد زايد[*1] ، خلود رمضان محمد عرابي[2] ، فاطمة صديق محمد[2]

١- قسم الكيمياء-كلية العلوم-جامعة القاهرة-الرقم البريدي ١٢٦١٣-الجيزة – مصر

٢- . قسم الكيمياء-كلية العلوم-جامعة أسوان-الرقم البريدي ٨١٥٢٨-أسوان-مصر.

في هذا البحث تم تحضير مشتق جديد لحمض المالينيليك (PNMA, p-nitrophenyl maleanilic acid) عن طريق تفاعل التكثيف بين مشتق الأنيلين (٤-نترونيلين) مع الماليك أنهيدريد بطريقة جديدة لاتحتوي علي مذيبات عضوية. كما تم تحضير بعض متراكبات الفلزات الانتقالية لمشتق حمض المالينيليك المحضرعن بتفاعله مع سداسي كربونيلات فلزات مجموعة الكروم الانتقالية وقد وضعت الصيغة الكيميائية الاتيه لهذه المتراكبات[$M(CO)_4L$] حيث (W, , L = PNMA, M = Cr M o) بنسبة (١: ١). كما تمت دراسة التركيبات الكيميائية لليجاند الحر PNMA ومتراكباته الجديدة من خلال التحليل االميكروئي ، التحليل الطيفي FTIR، ^{1}H-NMR ، التحليل الطيفي الشامل ، والتحليلات الحرارية TGA و DTGA. تم اختبار الهياكل الكيميائية لكل من الليجاندالحر PNMA ومتراكباته بواسطة XRD. تم دراسة النشاط المضاد للسرطان لكلا من الليجاند الحر و متراكب الكروم ضد خلايا MCF-7 (خلايا سرطان الثدي) ، خلايا HCT116 (خلايا سرطان القولون) وخلايا HepG2 (سرطان الكبد البشري).ووجد ان اللجند الجديدة المحضرة والمتراكبات العضو فلزية لها ذاتتأثير ملحوظ في معالجة وايقاف نشاط الخلايا السرطانية المذكورة.